SACLANTCEN REPORT
serial no: SR-269

SACLANT UNDERSEA RESEARCH CENTRE REPORT

OBSERVATIONS OF MEDITERRANEAN FLOW INTO THE BLACK SEA

D. Di Iorio, H. Yüce

October 1997

The SACLANT Undersea Research Centre provides the Supreme Allied Commander Atlantic (SACLANT) with scientific and technical assistance under the terms of its NATO charter, which entered into force on 1 February 1963. Without prejudice to this main task – and under the policy direction of SACLANT – the Centre also renders scientific and technical assistance to the individual NATO nations.

This document is approved for public release.
Distribution is unlimited.

NATO SACLANT Undersea Research Centre
Viale San Bartolomeo 400
19138 San Bartolomeo (SP), Italy

Tel: +39 187 540.111
Fax: +39 187 524.600

e-mail: library@saclantc.nato.int

NORTH ATLANTIC TREATY ORGANIZATION

Observations of Mediterranean flow into the Black Sea

Daniela Di Iorio and Hüseyin Yüce

The content of this document pertains to work performed under Project 022-1 of the SACLANTCEN Programme of Work. The document has been approved for release by The Director, SACLANTCEN.

Jan L. Spoelstra
Director

intentionally blank page

Observations of Mediterranean flow into the Black Sea

Daniela Di Iorio and Hüseyin Yüce*

Executive Summary: The Strait of Istanbul (Bosporus) separates the Black Sea and Marmara Sea each of which has different hydrological characteristics. The exchange of these waters through the strait is a classic example of turbulent exchange flow. The only exit of Black Sea water is through the Strait of Istanbul (Bosporus) and by evaporation. Fresh water input to the Black Sea is from rivers and precipitation; salt water input is of Mediterranean origin flowing through the strait. In order to understand the exchange process, the Black Sea hydrological characteristics and the resulting effect on acoustic surveillance systems, a detailed survey of the Black Sea exit region was carried out to determine the path and spreading extent of the dense Mediterranean water, the physical conditions that suppress the Mediterranean flow and the turbulent bottom boundary later characteristics associated with bottom friction. As the Mediterranean undercurrent is a strong flow, it is found that turbulent bottom velocity dominates the acoustic scattering for high frequency forward propagation systems. The spreading extent of the Mediterranean overflow water on the continental shelf (<100 m depth) can mask the effects of the sea bottom for short range acoustic backscatter systems and thus make it difficult to detect underwater objects. Future work in this area will concentrate on modelling the oceanographic variability for comparison with available environmental data.

* Eng. Capt. Assoc. Prof. Dr. Hüseyin Yüce, TUNA
Turkish National Represesentative, SACLANTCEN
Scientific Committee of National Representatives,
Head of the Department of Navigation, Hydrography
and Oceanography, Istanbul

intentionally blank page

Observations of Mediterranean flow into the Black Sea

Daniela Di Iorio and Hüseyin Yüce

Abstract:

Mediterranean Sea water inflow into the Black Sea is investigated using acoustic and oceanographic data obtained in the Black Sea exit region. The path of Mediterranean water and the resulting spreading on the continental shelf is observed with SWATH bottom bathymetry measurements, high resolution echo sounding images and conductivity, temperature and depth (CTD) profiles. It is found that the dilution of the saline Mediterranean water as it flows and spreads on the shelf is only 6.0 before reaching the continental slope where it sinks to a depth appropriate to its density. Temporal and spatial variability in the flow and their relation to atmospheric and sea level changes are documented. It is shown that blockage of the Mediterranean undercurrent occurs when the Black Sea water transport exceeds $25 \times 10^3\ m^3\ s^{-1}$ which corresponds to a relative sea level difference greater than 40 cm. Mediterranean flow into the Black Sea is a high Reynolds, low Richardson number flow resulting in a turbulent bottom boundary layer. Measurements of the path averaged turbulent kinetic energy dissipation rate give values ranging from 1×10^{-6} to $1 \times 10^{-4}\ W\ kg^{-1}$.

Contents

List of Figures

List of Tables

1

Introduction

The Strait of Istanbul (Bosporus) separates two relatively large inland seas of differing hydrological characteristics (see Fig. 1). Flow through the strait is a classic example of turbulent exchange flow (Tolmazin [1]). A high velocity surface current with relatively fresh Black sea water overlies a current running in the opposite direction, which transports the more saline bottom water of the Sea of Marmara which is of Mediterranean origin to the Black Sea. Highly saline and dense Mediterranean water flows through an underwater canyon which is an extension of the Strait of Istanbul (Bosporus) canyon until it spreads on the shelf at some 80 m water depth and finally reaches the shelf break and sinks to a depth at which it finds a common density.

The exchange through the Strait of Istanbul (Bosporus) plays an important role in determining the oceanographic properties in the neighbouring basins. The Mediterranean inflow is the only source of ventilation and renewal of anoxic waters of the deep Black Sea. The surplus of fresh water from rivers and precipitation against evaporation keeps the surface layer in the Black Sea relatively fresh and leads to higher outflow through the Bosporus than the average amount of saline Mediterranean water that advances into the Black Sea (see Ünlüata *et al.* [2]). This input/output process satisfies the salt balance within the Black Sea.

This paper describes oceanographic and acoustic measurements taken during a November/December 1995 sea trial to the Black Sea exit region. The measurement program was carried out as part of SACLANTCEN's Black Sea 1995 project in collaboration with the Turkish Navy Department of Navigation, Hydrography and Oceanography. An extensive data set was obtained and the analysis is divided into three main physical characteristics: path and spreading of Mediterranean water, blockage of the Mediterranean undercurrent, and the turbulent bottom boundary layer characteristics.

A number of studies have focused on the path and spreading extent of Mediterranean water on the Black Sea continental shelf (Ünlüata *et al.* [2], Yüce [3], [4] and Latif *et al.* [5]) because of its crucial role in the Black Sea salinity and water budgets. The main reason for the difficulty in tracking the Mediterranean water into the Black Sea has been lack of adequate information on the bathymetry and current measurements in the Northern entrance of the strait. The measurement technique described in this paper therefore differs extensively in that two dimensional imaging of the two layer

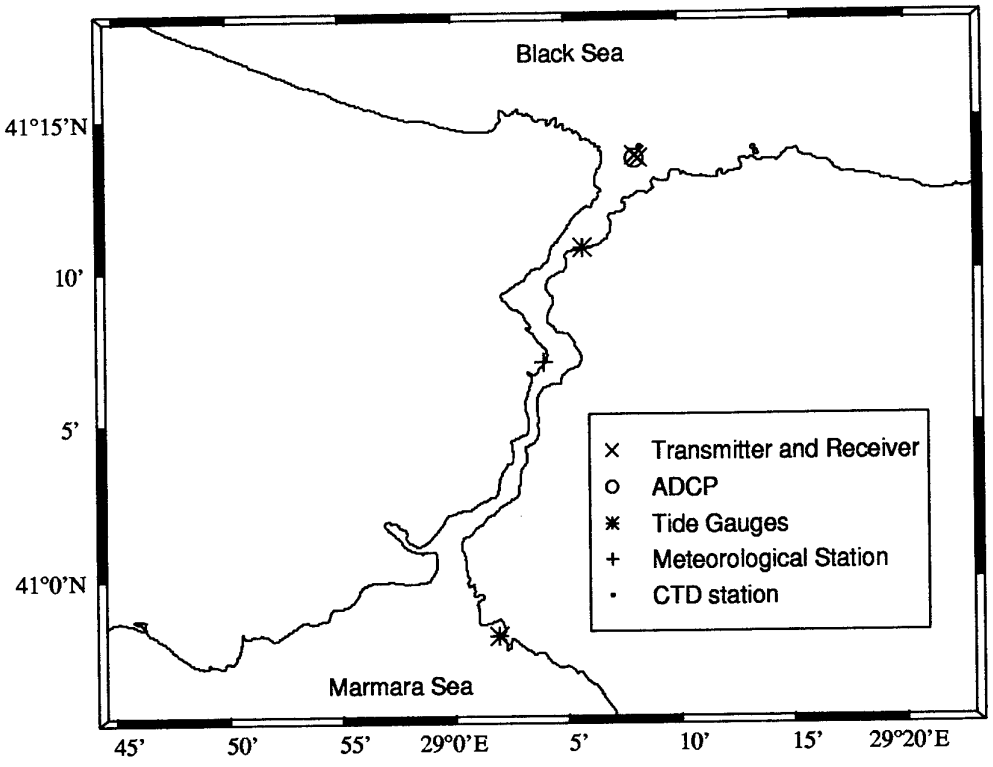

Figure 1 *Strait of Istanbul (Bosporus) showing the location of the acoustic Doppler current profiler, the acoustic scintillation transmitter and receiver, two tide gauges, a meteorological buoy and where TCG Çubuklu was stationed for CTD measurements.*

flow together with conductivity, temperature and depth (CTD) profiles are used to obtain a view of the flow pattern. Bathymetry, current and CTD measurements are obtained from the exit region of the Black Sea and the shelf area out to the continental slope.

Blocking of the Mediterranean flow into the Black Sea has also been a central area of study. Occasional blockage has been documented by Latif *et al.* [5] who observed complete but temporary (2 to 3 days) suppression of Mediterranean inflow. Modelling results of Oğuz *et al.* [6] show upper layer transport conditions which cause the lower layer transport to vanish. Our measurements in this paper make use of measured transport for each layer together with relative sea level difference measurements (which in turn depend on meteorological conditions and fresh water input) to show the intermittent nature of the Mediterranean flow over time scales of a few days.

The Mediterranean bottom boundary layer in the Black Sea exit and shelf region plays an important role in the exchange process as it determines the parameters of bottom friction; the mixing of quantities and the importance of friction on the flow are related to the intensity of the turbulence. In particular, the dissipation rate of the turbulent kinetic energy is also a measure of the turbulent energy levels. In this paper we make use of a high frequency acoustic scintillation system and the technique described by Di Iorio and Farmer [7] to estimate the turbulent kinetic energy dissipation rate and other bottom boundary layer parameters. Recent turbulence measurements were obtained along the Strait of Istanbul (Bosporus) (M. Gregg and E. Özsoy personal communication) and their measurements show strong levels of turbulence.

Section 2 describes the sea trial to the Black Sea exit region. The Mediterranean path and spreading is described in section 3; blockage is documented in section 4 and section 5 characterizes the turbulent bottom boundary layer. Conclusions are in section 6.

2

Experiment

The sea trial to the Black Sea exit region covered a period of 4 weeks in November/December 1995. The NATO Research Vessel (NRV) *Alliance* and the Turkish Navy Survey Ship (TCG) *Çubuklu* were the participating units of the research program. Initially, acoustic and oceanographic instrumentation were moored in the Strait of Istanbul (Bosporus) and at the exit region of the Black Sea (see Fig. 1). These instruments were used to monitor the exchange of Black Sea and Mediterranean Sea water. These instruments consisted of a high frequency (307 kHz) acoustic scintillation system for turbulence analysis and a 600 kHz broad band acoustic Doppler current profiler (ADCP) for flow and transport measurements. In addition, two sea level stations were placed at opposite ends of the Strait to give relative sea level difference data and a meteorological station monitored wind velocity and air pressure. In order to obtain temporal variability in temperature and salinity TCG *Çubuklu* was anchored for a 36 hour period obtaining CTD profiles every half hour and once an hour the CTD was lowered to 60 m depth to obtain a 12 min time series.

In studying this area an ATLAS multi-beam SWATH echo sounder was used to obtain detailed bottom bathymetry. For most of the experiment NRV *Alliance* and TCG *Çubuklu* surveyed the continental shelf, obtaining CTD profiles along the canyon and on a 3.5 km grid on the shelf so as to locate the Mediterranean effluent and measure the dilution. In addition, a high resolution, high frequency (120 kHz) echo sounder was used for two dimensional imaging of the two layer flow structure.

3

Path and Spreading

One basic element in studying Black Sea and Mediterranean Sea water exchange is knowing where the dense Mediterranean water finds its way along the shelf toward the slope and the resulting mixing that takes place with the cold intermediate water of the Black Sea. On the shelf the Mediterranean flow is expected to follow a 'delta' like structure and the salinity dilution is expected to occur quite rapidly compared to mixing and entrainment within the strait as will be discussed.

A detailed hydrographic survey with SWATH mapping was obtained in order to determine the path of the Mediterranean inflow into the Black Sea as available bathymetry was not sufficient. The results in Fig. 2 show that there is a narrow canyon extending from the Strait of Istanbul (Bosporus) in the Northeast direction which is an extension of the channel. Initially the canyon is parallel with the strait then turns to the Northwest where it eventually merges with the continental shelf. A 60 m sill exists within the canyon at its widest point. Mediterranean water is confined and retained within this canyon over a distance of several kilometres until it spreads out on the shelf. Simultaneous CTD profiles, from which sound speed is calculated, were obtained along the path of the underwater canyon in order to correct for the refracted lobes of the SWATH. No correction was made for instantaneous sea level measurements.

The flow of Mediterranean water is observed using a high resolution, high frequency (120 kHz) echo sounder towed along side either NRV *Alliance* or TCG *Çubuklu*. Figure 3 shows sample survey lines taken on the shelf where two dimensional imaging of the Mediterranean flow are observed. Knowing the bottom bathymetry, it was possible to make a transect along the canyon and then continue along the shelf where Mediterranean water was expected to flow. A number of cross sections along the canyon were also made in order to observe the spreading of Mediterranean water on the shelf. The 100 m contour line shown in Fig. 3 indicates approximately the start of the continental slope.

The acoustic characteristics and operating parameters for the Biosonics echo sounder are shown in Table 1. This same instrument was used by Armi and Farmer [8] and Farmer and Armi [9] in studying the exchange of Atlantic and Mediterranean Sea water through the Strait of Gibraltar. The narrow beamwidth together with the small pulse length and fast transmission rate allows high resolution measurements of

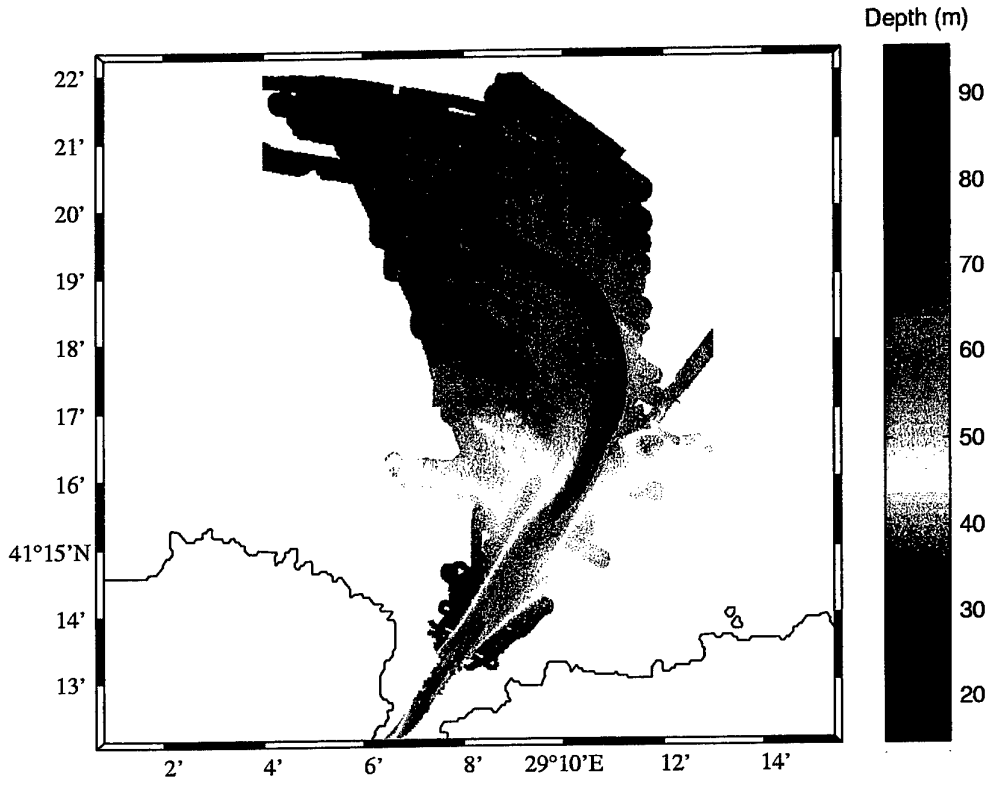

Figure 2 *Bottom bathymetry in the Black Sea exit region using the multi beam SWATH echo sounder.*

the two layer structure. Sound is scattered by small fish, zooplankton, and temperature/salinity microstructure.

Figure 4 shows a 35 km transect taken along the canyon from South to North with temperature profiles from expendable thermistors (XBTs) superimposed. The location of the profile is denoted by the marker o = 12 $^{\circ}C$. Since the depth of the echo sounding images is calculated based on a mean soundspeed profile, errors in the depth can be ± 2 m and this may explain why there is a vertical offset between some of the XBT profiles and the echo of the pycnocline. The temperature difference on average between the two water masses is 7 $^{\circ}C$ and the salinity difference is 18. The resulting density and sound speed difference is 14 $kg\ m^{-3}$ and 40 $m\ s^{-1}$ respectively.

The interface between Black Sea and Mediterranean Sea water is an area of intense turbulence associated with mixing of the two very different water masses. Biological matter distributed at the interface together with the turbulence gives strong acoustic

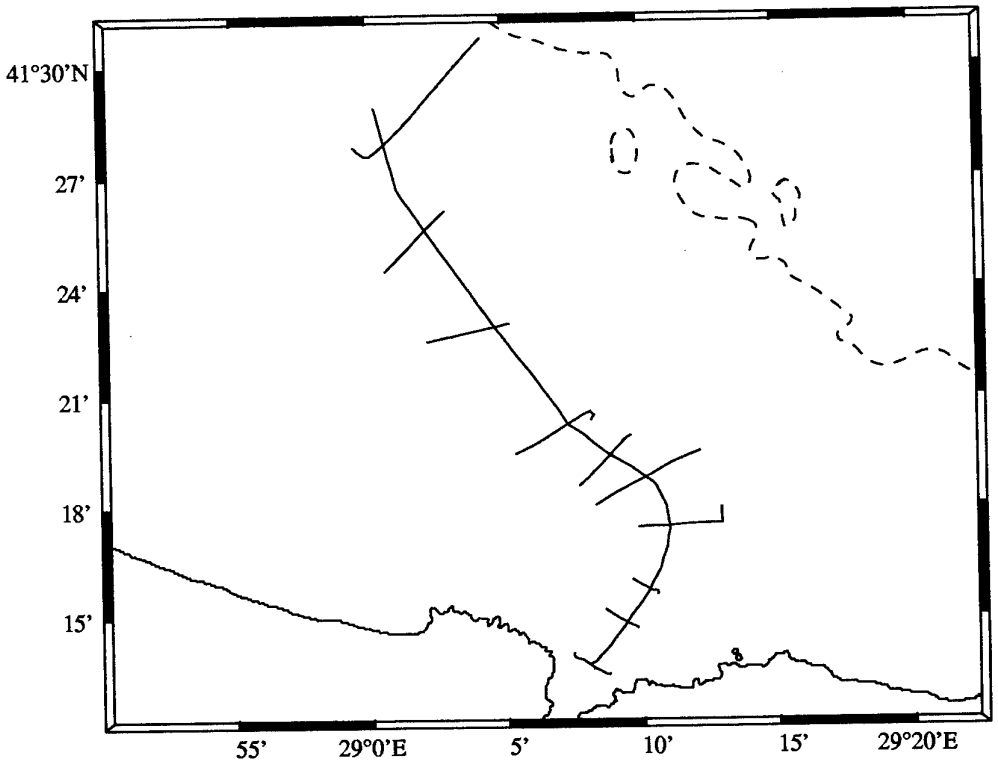

Figure 3 *Ship transects along and across the canyon where high resolution echo sounding images were obtained. The continental slope starts approximately at the 100 m contour (dashed line).*

back scatter characteristics. Measurements show that the normal incidence echo level from the interface is 40% that of the bottom reflection. Much structure is visible at the interface which suggests strong spatial variations associated with turbulent mixing along the canyon.

The 60 m sill located 3 km from the entrance to the Strait of Istanbul (Bosporus), is a hydraulic control for Mediterranean flow into the Black Sea. Oğuz *et al.* [6] studied the nature of the two layer exchange by examining composite Froude number variations along the Strait. The composite Froude number for a two-layer channel flow (see Farmer and Armi [9]) is defined by,

$$G^2 = F_1^2 + F_2^2 \quad (1)$$

$$F_i^2 = U_i^2/g'h_i \quad (2)$$

where subscripts $_1$ and $_2$ refer to the upper and lower layer respectively, $g' = (\rho_2 - \rho_1)g/\rho_2 \approx 0.14\ m\ s^{-2}$ is the reduced gravity, U is the flow speed and h is the layer thickness. At the sill location the Black Sea upper layer is not constrained by

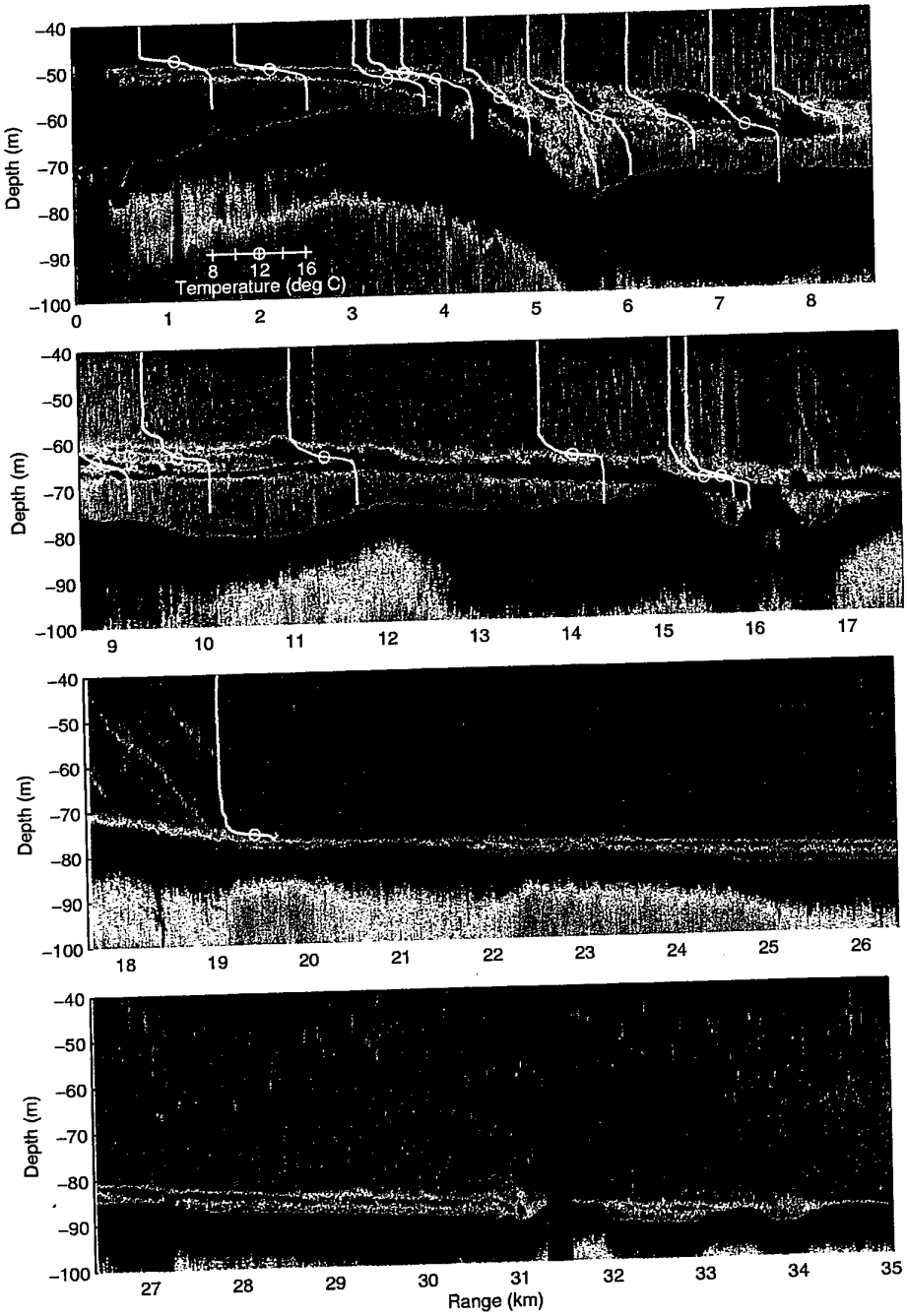

Figure 4 *Acoustic back scatter images taken over a 35 km transect along the canyon and continental shelf. Temperature profiles from XBTs are superimposed so that the marker $o = 12\ ^{\circ}C$ represents the location.*

Parameter	quantity
Frequency	120 kHz
Source level	215.3 dB re $1\mu Pa$ @ 1 m
Beam width	3.8^o
Pulse width	0.2 ms
Transmission interval	0.2 (sometimes 0.3 s)
Time variable gain	$20 \log r$

Table 1 *Towed echo sounder instrument parameters.*

the channel and so the flow is considered a single layer reduced gravity flow. It is anticipated that the flow of the lower layer is controlled over the crest of the sill ($F_2^2 = 1$). South of the sill the flow must then be subcritical ($F_2^2 < 1$) and North of the sill it must be supercritical ($F_2^2 > 1$).

Measurements from the moored ADCP and CTD profiles obtained south of the sill (as will be shown) give a Froude number $F_2^2 = 0.1$ which is < 1. North of the sill the density current plunges down the sill slope causing the Mediterranean layer to become turbulent. Proceeding further northward the Mediterranean layer restratifies. As the Mediterranean water flows onto the shelf it becomes very thin as a result of spreading and is expected to follow a 'delta' like structure.

Echo sounding cross sections along the canyon at locations [0.1 3.2 5.2 8.7 11.3 13.7 16.3 22.5 28.4 33.5] km in Fig. 4 are shown in Fig. 5. Some of the cross sections are taken at different times compared to the along canyon measurement. However, all images were taken during a time when the Mediterranean inflow was strong. The depth covers 60 m and are to scale from image to image but the horizontal distances are not to scale and vary. Ten images are shown corresponding to the southernmost transect first and the northernmost transect last of Fig. 3. The range is set so that 0 km corresponds to the location where the along canyon transect was taken; negative (positive) range values thus correspond to the distance left (right) of the along canyon transect.

The first image of Fig. 5 is a cross section south of the sill where the ADCP and acoustic scintillation instruments were moored and where the flow is subcritical. Also shown next to the image is a sample density profile which shows that the interface is made up of two distinct mixing regions. The second image is taken across the sill. North of the sill the flow is supercritical and recent measurements from a 1996 survey showed flow speeds exceeding 1 $m\ s^{-1}$ thus causing the entire Mediterranean layer to become fully turbulent.

The fourth and fifth images are taken where the canyon turns to the Northwest. Because of channel curvature there is a cross channel circulation that causes Mediterranean water to accumulate on the right thus spilling over the canyon edge. As

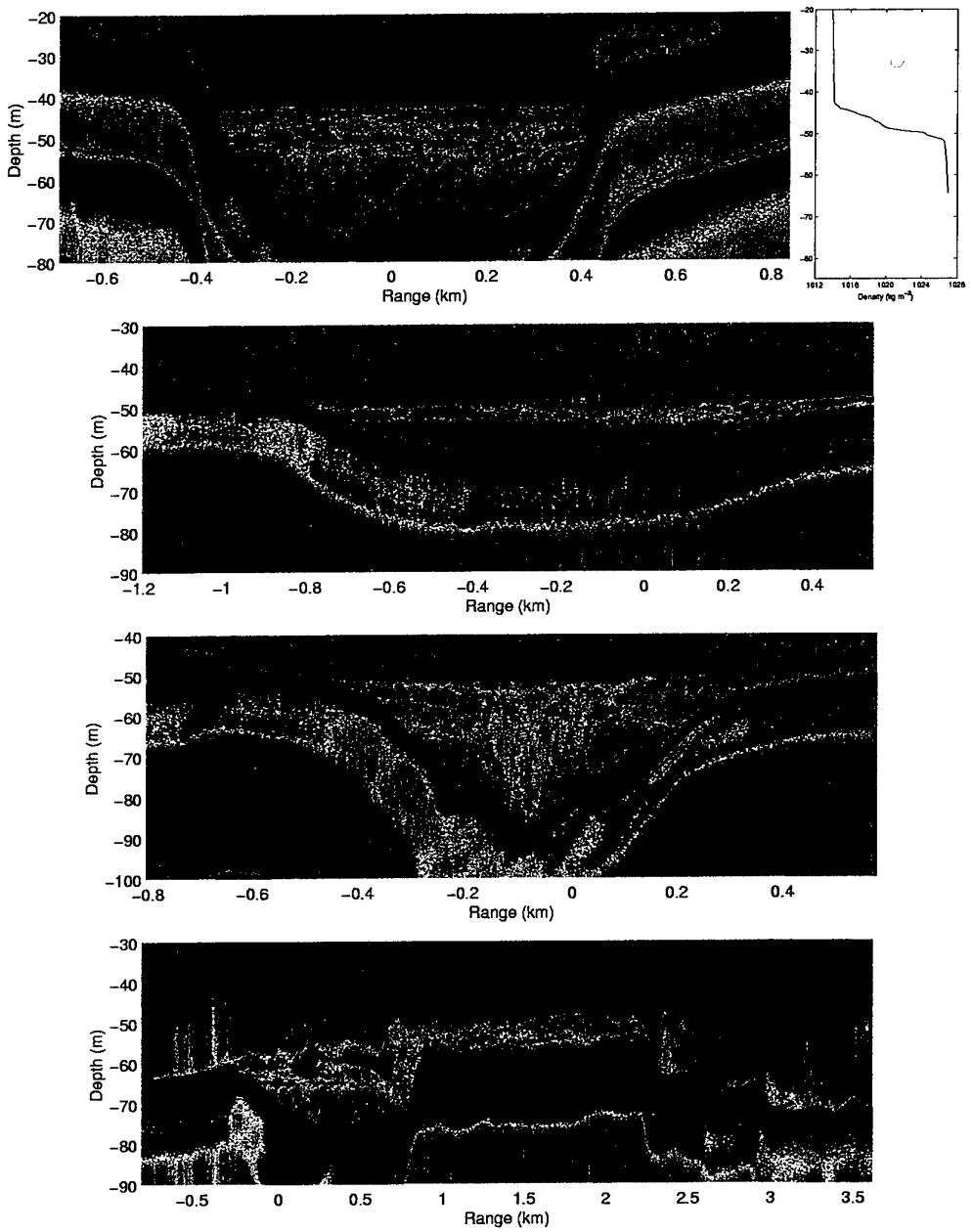

Figure 5 *Acoustic back scatter images taken across the canyon and shelf. A sample density profile is shown for the first image. Images are from the southernmost cross section to northernmost and are located at [0.1 3.2 5.2 8.7 11.3 13.7 16.3 22.5 28.4 33.5] km in Fig. 4.*

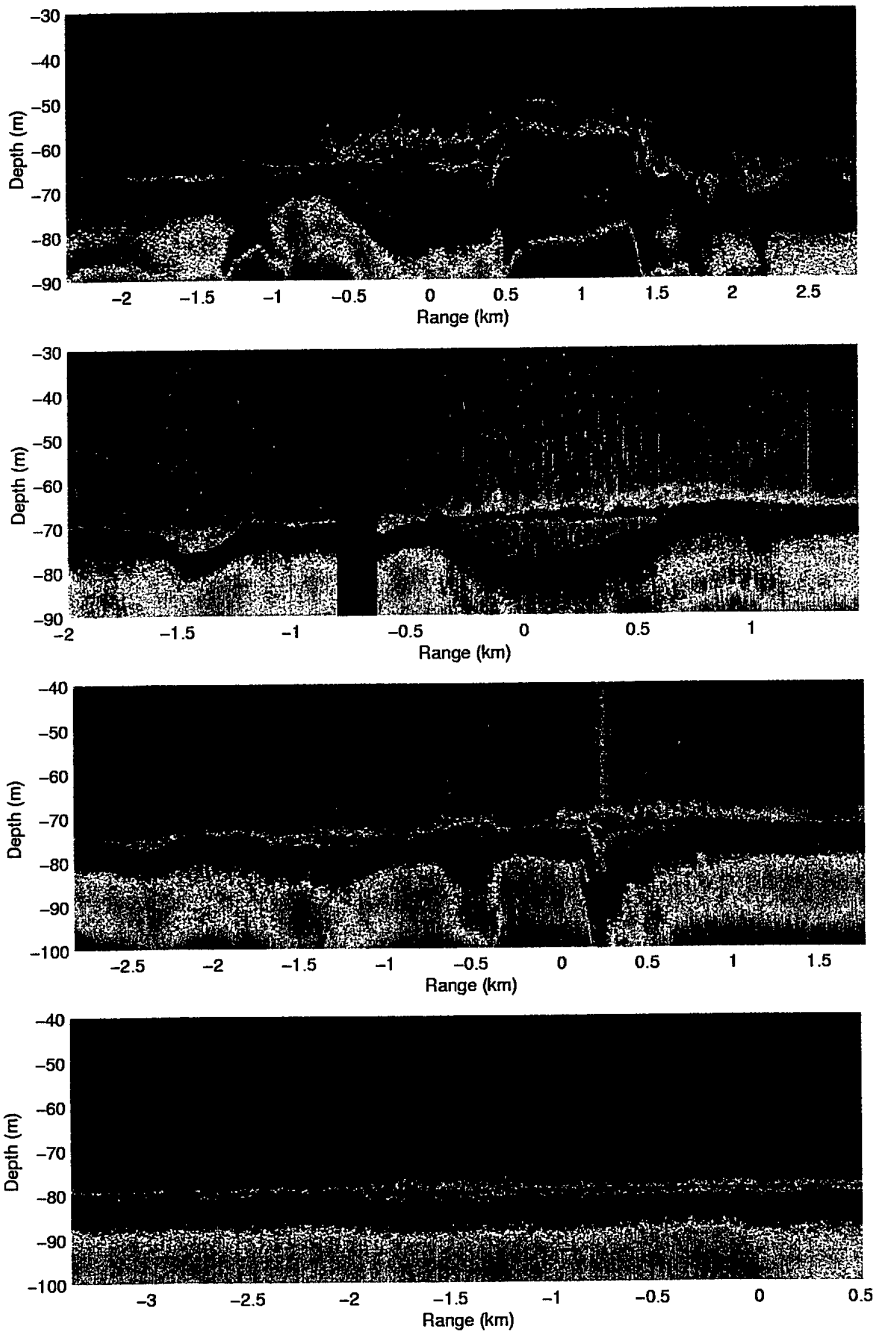

Figure 5 continued.

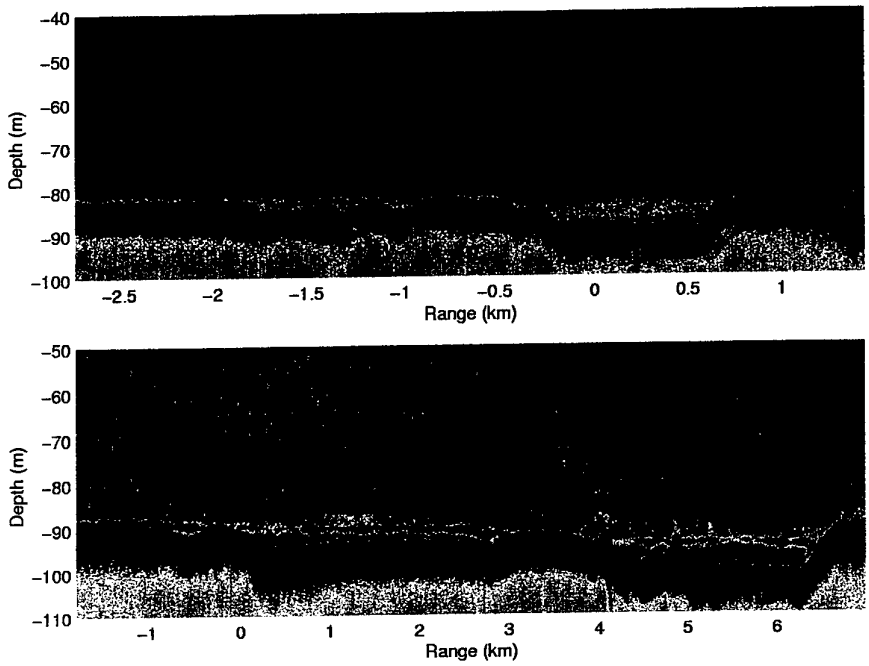

Figure 5 continued.

the flow enters the bend, surface Mediterranean water moves to the outside of the bend, and saltier water from below is brought to the interface on the inside of the bend. This flow structure within the Mediterranean layer thus causes intense vertical mixing and needs to be confirmed with further observations.

Spreading of the Mediterranean effluent has filled adjacent canyons to the left of the main canyon as seen by the fifth, sixth and seventh image. As the canyons merge with the shelf, the Mediterranean effluent spreads horizontally as seen by the eighth image. Finally the last two images correspond to cross sections taken just prior to the continental slope. These images show the presence of two main shallow canyons filled with the effluent.

To observe the spreading extent of the Mediterranean water and thus its path along the continental shelf, a series of CTD profiles from NRV *Alliance* and TCG *Çubuklu* were obtained. In addition to profiles taken along the canyon, a 3.5 km grid of CTD profiles were also obtained in order to cover the shelf and part of the slope area. When there were good weather conditions, it was possible to sample the water column close to the bottom in order to determine the Mediterranean characteristics. With these measurements, the highly saline water was followed over several kilometres and its dilution with overlying Black Sea water observed. The dilution of the effluent is

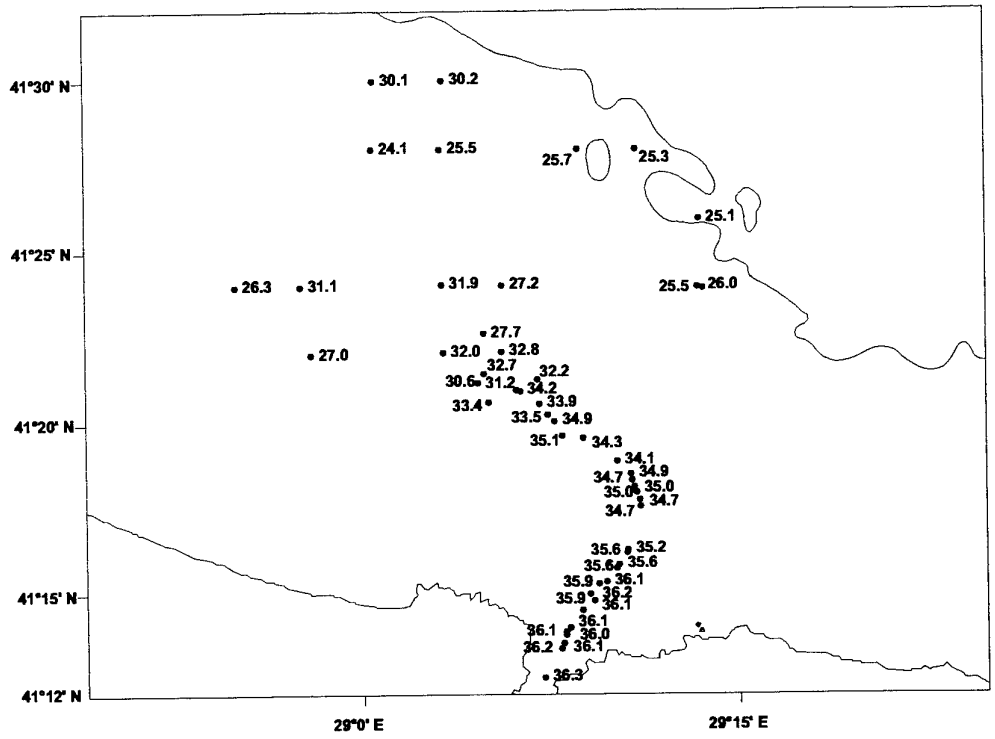

Figure 6 *Bottom salinity values greater than 24.*

expected to occur quite rapidly beyond the sill because of supercritical flow, channel curvature and thinning of the layer to a few metres.

Figure 6 shows the location of bottom salinity values greater than 24 which indicate the presence of Mediterranean water; the salinity of the deep Black Sea water is 22.3. On the shelf, the Mediterranean layer spreads to a few metres thick and it is possible that some of the CTD profiles did not reach the bottom Mediterranean water. Nevertheless, the extent of the spreading and the path of the Mediterranean inflow can be seen by the figure.

Measurements show that the dense water enters the Black Sea with a salinity of 36. According to Ünlüata *et al.* [2] the Mediterranean enters the Strait of Istanbul (Bosporus) from the Marmara Sea with salinity 37. Thus, during its passage of 35 km through the Strait the water is diluted to 36. As the Mediterranean water makes its way along the canyon of the Black Sea the salinity drops to 33, a reduction of 3 over a 20 km path. The dilution is expected to continue quite rapidly on the shelf until it finally reaches the continental slope. At the 100 m contour Latif *et al.* [5] observed salinities ranging between 20 and 22. Our measurements show salinities of

25 and 30 close to the 100 m contour. These high salinity values imply the formation of a water mass dense enough to sink to, and hence cause renewal of, the deep Black Sea water.

4

Flow Characteristics

An acoustic Doppler current profiler was bottom mounted at depth 72.2 m looking upwards within the canyon south of the sill (at the 0.1 km range of the first cross canyon image of Fig. 5). Table 2 lists the relevant set up parameters. The ADCP transmits once every 12 s and obtains a 40 transmission ensemble average every 10 min. Three components of current are obtained: N-S, E-W and vertical at 1 m bin intervals for 50 bins. The physical characteristics of this instrument allow measurement close to the bottom boundary (the first sample is 2.2 m from the bottom).

As the ADCP is confined within the canyon oriented approximately 38° from True North, the component of flow (U) resolved along this direction is shown in Fig. 7. White is used to denote zero current. Positive values correspond to flow toward the North. In order to maintain a right handed coordinate system the (x,y) axes are aligned with the along and cross canyon direction which corresponds approximately to the Northeast and Northwest respectively. Maximum Mediterranean Sea water inflow is 0.8 $m\ s^{-1}$ occurring between depths 50 and 60 m, and maximum Black Sea outflow is $-0.3\ m\ s^{-1}$ over the entire layer. The most striking feature of this two layer flow dynamics is the temporal variability of the Mediterranean flow over a time scale of 6 days.

The streamwise shear (dU/dz) is also shown in Fig. 7. Over the 1 m bin separation the maximum shear observed is $-0.5\ s^{-1}$. The shear is used as a sensitive measure-

Parameter	quantity
Start time	26-NOV-1995 13:04 UTC
End time	13-DEC-1995 11:34 UTC
Frequency	600 kHz
Transmission rate	0.08333 Hz
Ensemble average	40 transmissions
Ensemble interval	10 min
Bin length	1 m
Total bins	50
Depth range	21 to 70 m

Table 2 *Bottom mounted ADCP instrument parameters.*

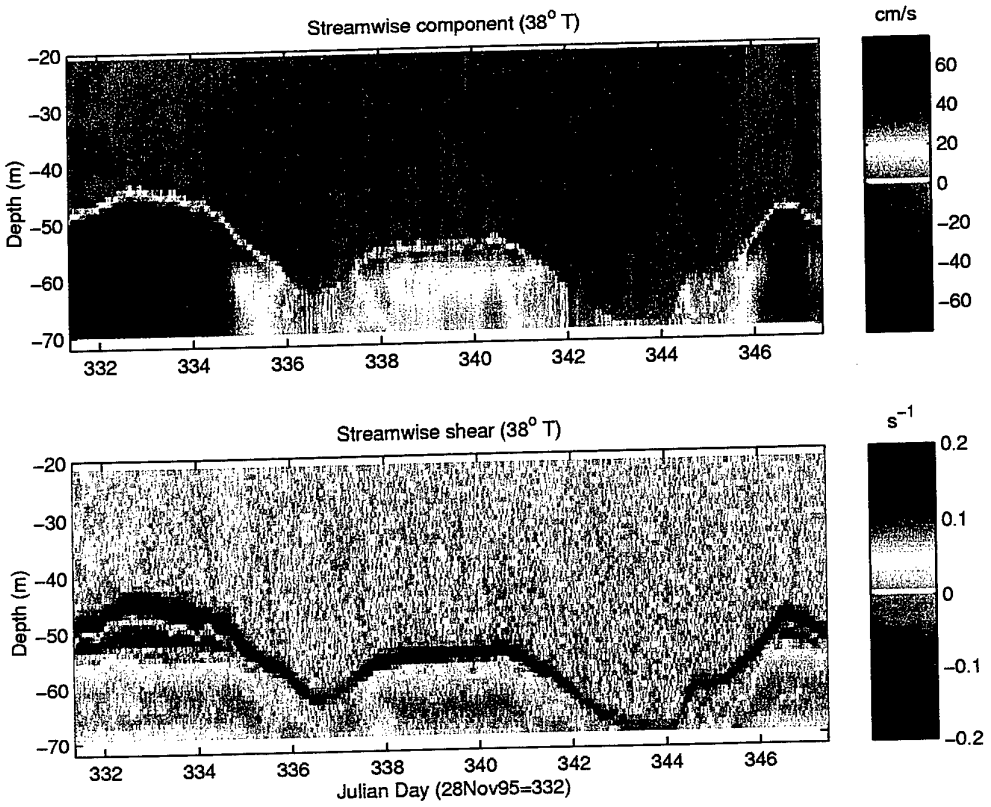

Figure 7 *The component of flow and shear resolved along 38° True North. Mediterranean flow into the Black Sea (Northeast) is positive.*

ment of the interface depth which is shown in Fig. 8. The sill depth of 60 m is also shown as a dotted line. The measurement shows that the Mediterranean flow is blocked by the sill since the interface drops below the sill depth.

Volume transport as a function of time can be estimated from the current measurement resolved along the direction 38° True, and flow geometry for each water mass. The depth averaged velocity is computed for each layer, and the transport is calculated based on the dimensions of the canyon and the strait. As the upper layer is not confined by channel width as the lower layer, we make an estimate of the transport based on an extension of the strait. On average the width of the canyon is $W_c = 700$ m at the ADCP location and the width of the Strait at the exit region is approximately $W_s = 3700$ m. The canyon depth is 72 m and the sea bottom outside the canyon is at a depth of 28 m (see the first image of Fig. 5). Mathematically the volume transport in the x direction for each layer is,

$$Q_{xM} = W_c \int_{-72}^{H} U dz \qquad \text{Mediterranean layer} \qquad (3)$$

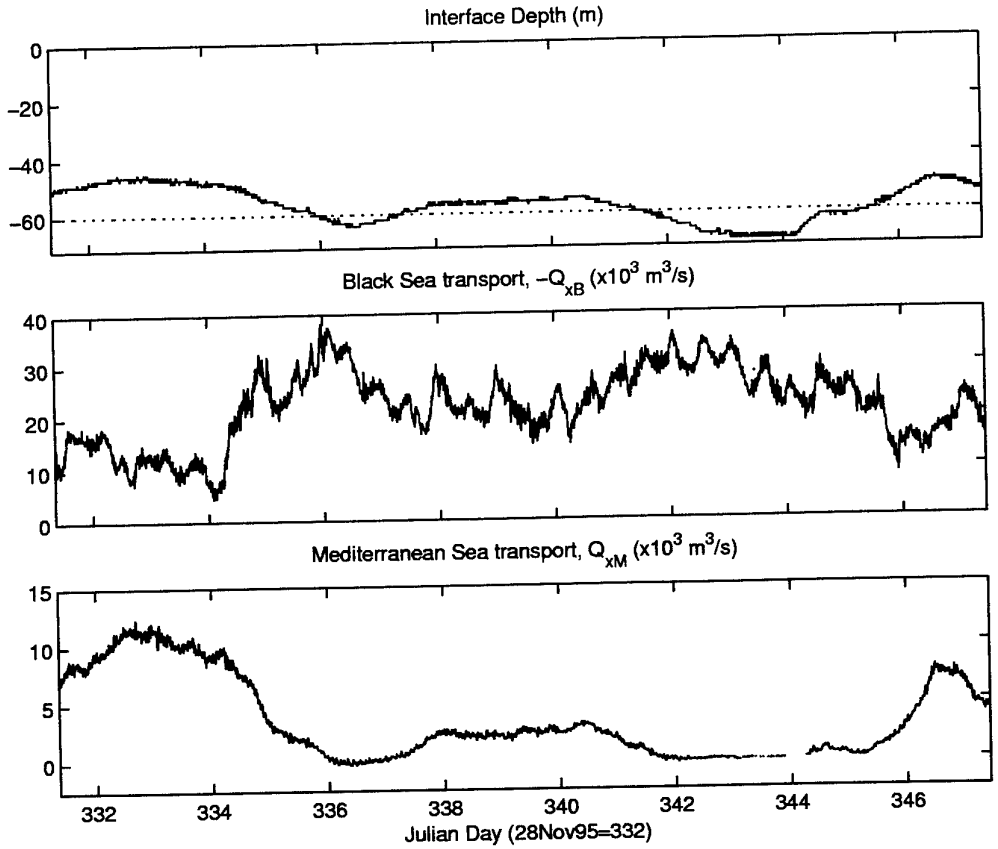

Figure 8 *The interface depth (solid curve), the sill depth (dotted curve) and the transport of Black Sea and Mediterranean Sea water.*

$$Q_{xB} = W_c \int_H^{-28} U dz + W_s \int_{-28}^{0} U dz \qquad \text{Black Sea layer} \tag{4}$$

where H is the interface depth and subscripts $_M$ and $_B$ correspond to the Mediterranean and Black Sea layers respectively. The estimated volume transport results Q_{xM} and $-Q_{xB}$ are shown in Fig. 8.

As expected, the Black Sea outflow is always greater than the Mediterranean inflow except during intense Mediterranean flow on Julian day 333 (29/11/95) when they are nearly balanced. When there is lower layer blockage there is extreme Southwesterly flow in the upper layer and when there is upper layer blockage there is intense Northeasterly flow in the lower layer. When the interface drops below the sill depth the Mediterranean transport ceases.

The blockage characteristics are related to the sea level difference between the Black Sea and Marmara Sea, which in turn depend on wind speed, barometric pressure

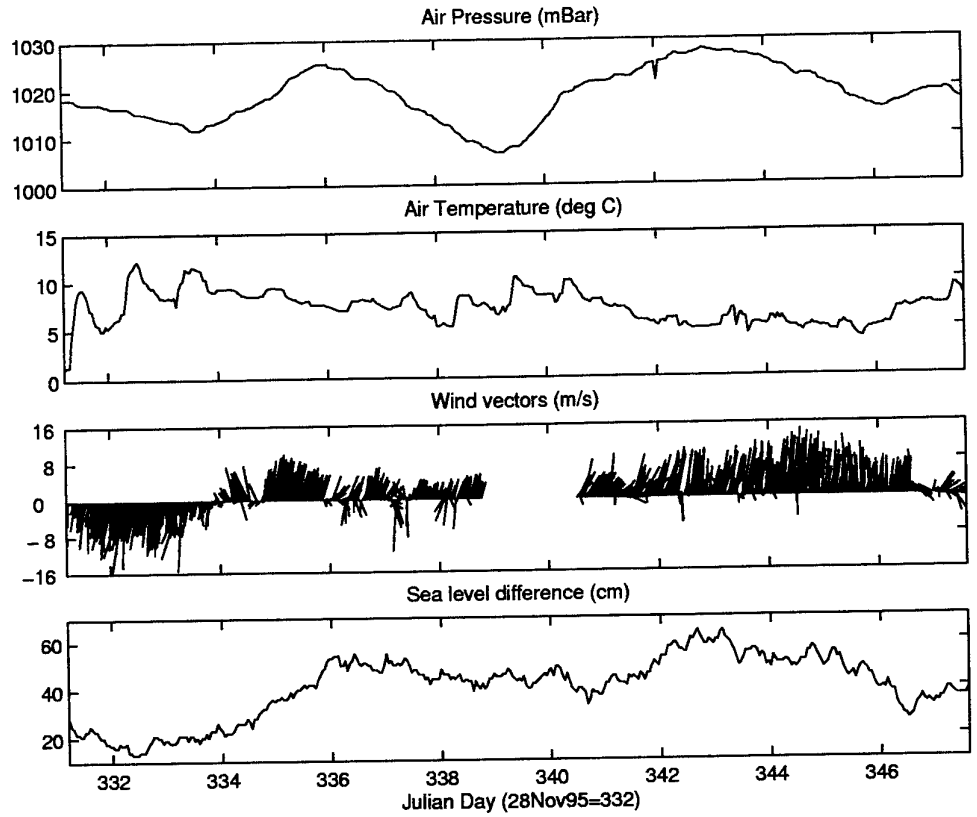

Figure 9 *Meteorological data showing air pressure, temperature, wind speed, direction and relative sea level difference.*

and freshwater input (see Yüce [10]). Meteorological data with relative sea level difference during the experimental period are shown in Fig. 9. As the wind speed from the meteorological station showed low values (the placement was in a sheltered area), data from the Meteo system on board NRV *Alliance* is used. Strong winds ($\approx 10\ m\ s^{-1}$) were observed during the experimental period in the Black Sea exit region.

The period of intense Mediterranean inflow and thus weak Black Sea transport is related to the strong southerly winds. When the winds change direction on Julian day 334 (30/11/95) the Black Sea transport approaches zero. For the duration of the experiment strong Northerly winds were observed resulting in relative sea level differences exceeding 40 cm which in turn causes Black Sea transport to exceed $25 \times 10^3\ m^3\ s^{-1}$. These conditions result in Mediterranean blockage and the results are consistent with the modelling conclusions of Oğuz *et al.* [6]. Time delays between blockage and sea level differences may exist because of the response time required for

the water masses to react to meteorological changes.

Since Mediterranean flow is confined between two boundaries (the bottom boundary below and Black Sea water above), a balance of friction, Coriolis force and pressure gradient will result in a cross stream shear over the full thickness of the Mediterranean layer. The governing equations for flow with friction are,

$$fV + F_x - \frac{1}{\rho}\frac{dP}{dx} = 0, \tag{5}$$

$$-fU + F_y - \frac{1}{\rho}\frac{dP}{dy} = 0, \tag{6}$$

where f is the Coriolis parameter, F is the frictional force along the x and y direction, P is the pressure and ρ is the density.

Figure 10 shows profiles of the along and cross stream current components (a right handed coordinate system: z positive upward, U positive northward and V positive westward) averaged over 1.2 days when the Mediterranean flow was maximum (between Julian day 332 6:35 and 333 10:54). The current vectors as a function of depth are also shown but plotted so that West is to the left and East is to the right thus maintaining a right handed coordinate system. As the bottom boundary is approached, the current speed decreases as a result of bottom friction and thus the Coriolis force to the right (East) decreases; the pressure gradient to the left (West) remains the same and thus the current swings to the left i.e. West. This balance of forces results in an Ekman spiral. A similar argument can be applied to the Mediterranean flow as it approaches the interface. Interfacial friction slows the current thus decreasing the Coriolis force. The constant pressure gradient to the left causes the current to also swing to the West.

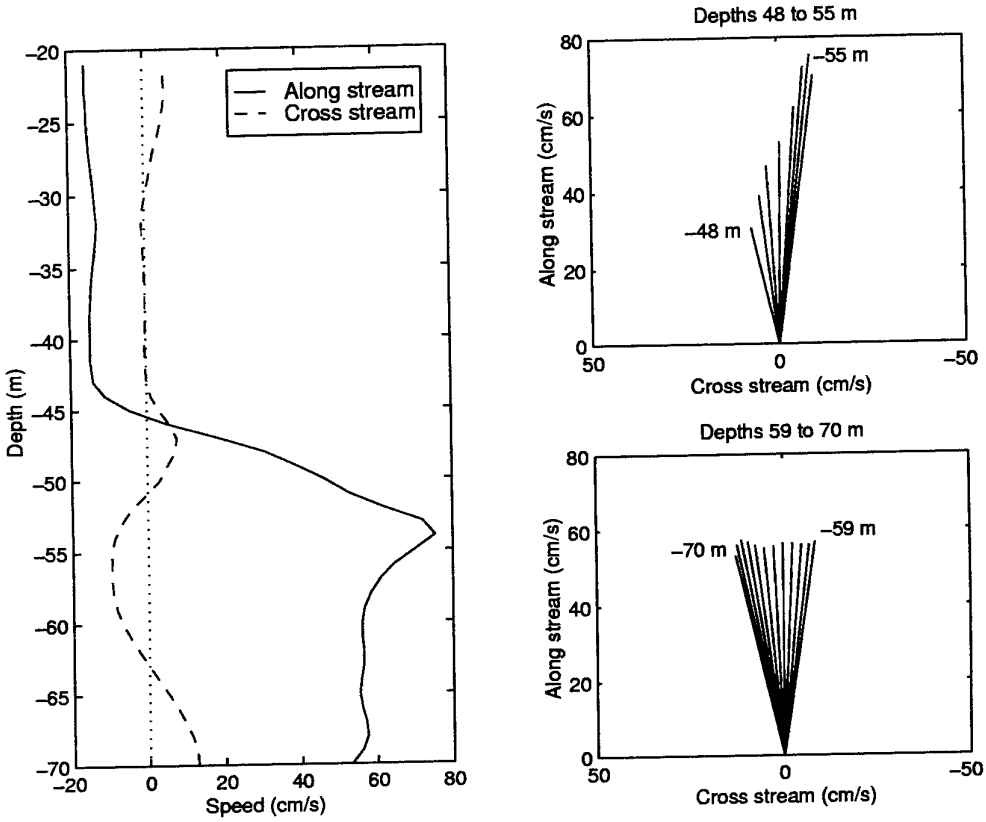

Figure 10 *Averaged profiles for the along and cross canyon current components with current vectors for depths 48 to 55 m and 59 to 69 m. Positive U and V corresponds to a right handed coordinate system.*

5

Turbulence parameters

The CTD time series at the anchored station near the ADCP and acoustic scintillation system (see Fig. 1) consisted of profiles approximately every half hour. The CTD was deployed once an hour at 60 m depth for a 12 minute time series of oceanographic properties. This temporal variability in temperature and salinity structure is used to determine the amount of mixing that takes place between the two layers. The 60 m depth was chosen to correspond with the acoustic propagation axis of the scintillation system.

Figure 11 shows contours of density superimposed on ADCP vector data. Times correspond to turbulence measurements made from the acoustic scintillation system, as will be discussed. During the CTD time series period ($\approx$ 36 hours) the interface had increased in thickness by 4 m as a result of mixing. Some of this mixing may occur at location or changes in the hydrological properties may be due to advection of mixed water from elsewhere. Also, the 1014 $kg\ m^{-3}$ density contour becomes shallower indicating that the Black sea layer at this location had a gain of salt by turbulent entrainment, or saltier water was advected from the Black Sea. Similarly, a decrease of salt content in the Mediterranean effluent occurs as the 1026.75 $kg\ m^{-3}$ contour deepens.

To calculate the amount of salt gained in the Black Sea layer at this location (and also lost in the Mediterranean layer) the depth averaged salt content is evaluated for each. The interface is arbitrarily identified as the depth at which the salinity becomes greater than or equal to 30. The change in the depth averaged salinity from initial values is shown in Fig. 12. Over the 36 hour period when the Mediterranean inflow was at its greatest, a mean salinity increase of 0.4 [psu] was observed; the lower Mediterranean layer shows a mean salinity loss on average of 0.6 [psu].

The CTD profiles together with the current profiles from the ADCP give a measure of hydrodynamic stability. This is parameterized by the gradient Richardson number (see Monin and Ozmidov [11]),

$$\mathrm{Ri} = N^2 \left[\left(\frac{dU}{dz} \right)^2 + \left(\frac{dV}{dz} \right)^2 \right]^{-1}, \tag{7}$$

$$N^2 = -\frac{g}{\rho_o} \frac{d\rho_o}{dz}.$$

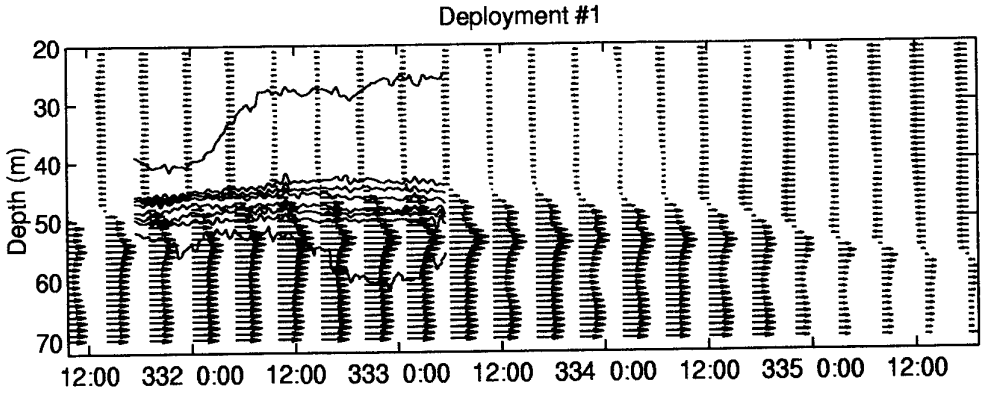

Figure 11 *ADCP current vectors (with density contours [1014, 1015, 1017, 1019, 1021, 1023, 1025, 1026.75] kg m^{-3} when available) during the time when acoustic scintillation data were obtained.*

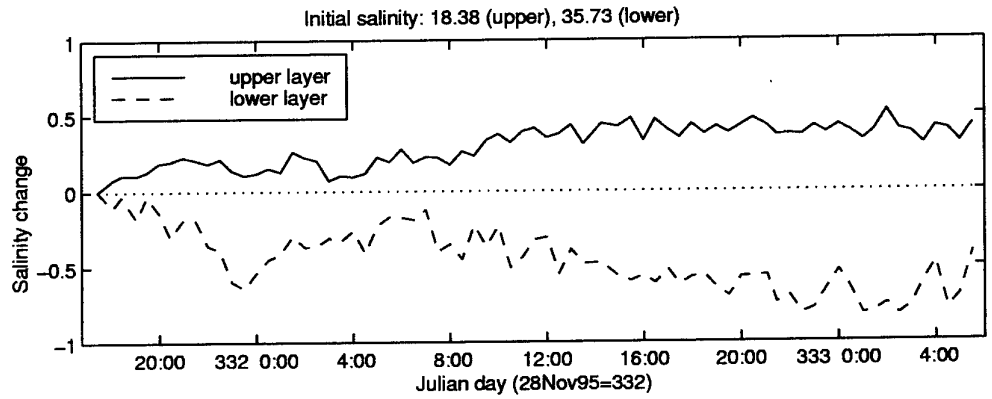

Figure 12 *The change from initial values in the depth averaged mean salinity for the Black Sea (upper) and Mediterranean Sea (lower) layer.*

where the mean flow as a function of depth resolved along and across the canyon is U and V respectively. The Brunt-Vaisala frequency is $N/(2\pi)$, ρ_o is the mean density as a function of depth and g is gravity. If the stratification is unstable, Ri < 0 then density variations enhance the turbulence. If the gradient Richardson number becomes large then turbulence is suppressed since the density gradient stabilizes the variations caused by the current shear (Monin and Ozmidov [11]). From our time series measurements we find that throughout the Mediterranean layer the Richardson number was consistently $0 <$ Ri $< 1/4$ indicating hydrodynamic instability.

The turbulence is also parameterized by the Reynolds number,

$$\mathrm{Re} = \frac{UL}{\nu}, \tag{8}$$

where the Mediterranean thickness is the scaling length L and ν is the kinematic viscosity. Measurements give a Reynolds number of the order of 2×10^7 during the time of intense inflow.

To measure the turbulence intensity, a high frequency (307.2 kHz) acoustic scintillation system was deployed within the canyon containing Mediterranean sea water. This instrument is self contained and battery operated with specifications given by RD Instruments [12]. The transmitter array was deployed on the western side and the receiver array on the eastern side separated by 280 m at a depth of 62.5 m. Each array consists of two transducers separated by 0.2 m. In order to keep the transducer array aligned in the direction of flow, a vane and swivel were attached to the mooring. This allows measurement of current flow perpendicular to the acoustic axis and measurement of turbulent structures as they are advected past the acoustic path.

Each transducer is horizontal omni-directional with a 10^o vertical beam width. Short pulses (30 cycles or 0.1 ms) are transmitted with a high repetition rate (16 Hz) and with a delay of 20 ms between the two spatially separated transducers. The receiver unit complex demodulates the signals, digitizes and calculates the acoustic amplitude, phase and travel time for the direct path using quadratic interpolation of the received envelope. The data are then recorded on flash EPROM recorder cards. Table 3 summarizes the experimental parameters.

In order to calculate the amplitude, phase and travel time of the acoustic pulse, it is crucial that there is path separation at the receiver. For example, ray tracing with a source and receiver at 62.5 m depth having vertical beam width of 10^o and separated by 280 m shows that there are only two paths: a direct path and a bottom reflected path. The time separation between the two paths is 0.45 ms and since the pulse length is 0.1 ms, path separation is possible.

Sample acoustic scintillation data (approximately 2 min of amplitude and travel time difference fluctuations) taken when the Mediterranean undercurrent is strong and when it is weak are shown in Fig. 13. Considerable variability in the amplitude

Parameter	quantity
Start time	27-NOV-95 11:00 UTC
End time	01-DEC-95 17:00 UTC
Transmission rate	16 Hz
Frequency	307.2 kHz
Pulse width	0.1 ms
Pulse delay	20 ms
Digitization rate	153600 Hz (1 sample/2 cycles)
Path length	282 m
Fresnel length $\sqrt{\lambda L}$	1.2 m
Propagation direction	124° True
Transducer separation	0.2 m
Depth	62.5 m

Table 3 *Acoustic scintillation instrument parameters.*

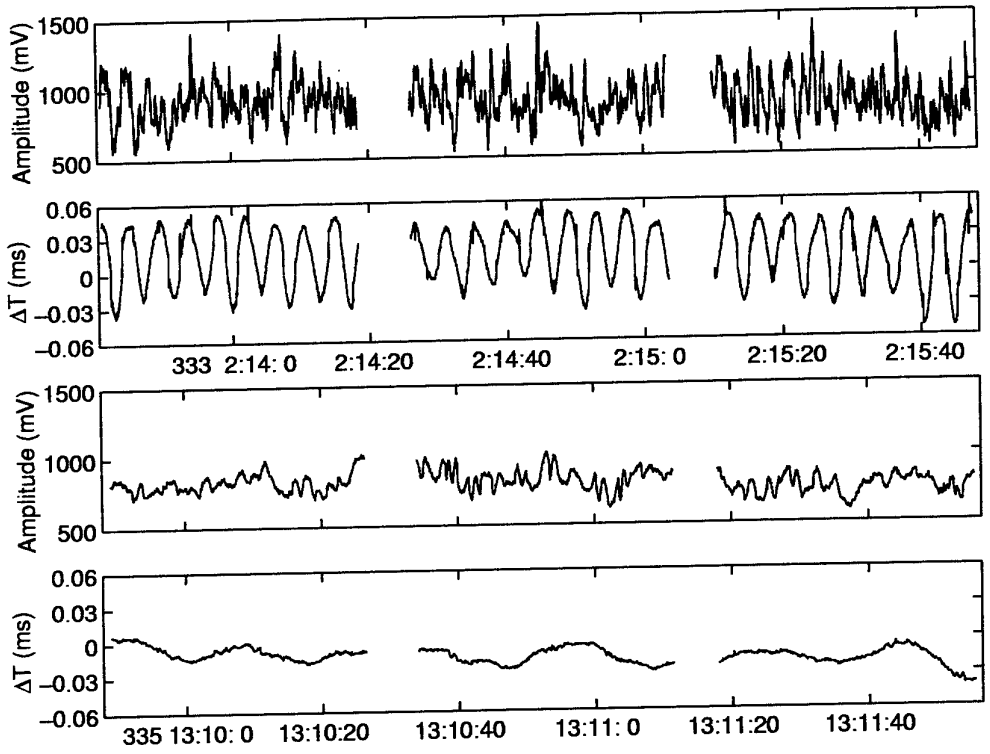

Figure 13 *Sample acoustic scintillation data when the Mediterranean undercurrent was strong ($U = 0.6\ m\ s^{-1}$ on Julian day 333 2:14) and weak ($U = 0.1\ m\ s^{-1}$ on Julian day 335 13:10).*

during strong flow is due to the turbulent nature of the flow. The travel time difference between the two parallel paths shows a periodic nature as a result of mooring oscillations. During weaker flow, the amplitude fluctuations and the periodicity in the travel time difference become less pronounced. As the transmission rate was high (16 Hz) and the mooring oscillations small, the direct path signal could be tracked. The mooring motion does not affect amplitude variations but the phase hence travel time cannot be used as a measurement of medium properties.

From the theory of wave propagation through random media given by Tatarskii [13], the statistics for the normalized log-amplitude $\chi = \ln(A/ < A >)$ (where A is the acoustic amplitude and $<>$ denotes a time average), allow measurement of oceanographic parameters (see for example Farmer *et al.* [14] and Di Iorio and Farmer [7]). Measurement of the log-amplitude from the two parallel acoustic paths gives a time-lagged cross-covariance function which corresponds to the translation of turbulent structures perpendicular to the two acoustic paths separated by 0.2 m. By measuring the time lag, the current speed is calculated and shown in Fig. 14 together with the ADCP measurement for comparison. Discrepancies between the scintillation technique and the ADCP can arise for a number of reasons. For example, the scintillation measurement is a path average whereas the ADCP measurement is essentially a volume measurement at a point location. Also because of mooring motion, there are changes in the acoustic path separation of 0.2 m.

The level of the effective refractive index fluctuations defined by,

$$C^2_{n_{eff}} = C^2_{n_s} + \frac{11}{6} C^2_{n_v} \tag{9}$$

(see Ostachev [15] and Di Iorio and Farmer [16]) is expressed in terms of the refractive index fluctuations arising from temperature and salinity variability (scalars) and those arising from current variability (vectors). The three-dimensional wave number spectrum for the effective refractive index fluctuations is described by the Kolmogorov spectrum,

$$\Phi_{n_{eff}}(K) = 0.033 C^2_{n_{eff}} K^{-11/3}, \tag{10}$$

for isotropic and homogeneous turbulence. The log-amplitude variance (assuming weak scattering of the acoustical signal, $\sigma^2_\chi << 0.25$) allows measurement of $C^2_{n_eff}$ through the equation,

$$\sigma^2_\chi = 0.124 C^2_{n_{eff}} k^{7/6} L^{11/6}, \tag{11}$$

where k is the acoustic wavenumber and L is the acoustic path length. The results are shown in Fig. 14. Note that the acoustic amplitude variability cannot distinguish between fine scale variability from scalars and that from current. The dominant scale size which contributes to the log-amplitude variance as discussed by Tatarskii [13] is the Fresnel radius $\sqrt{\lambda L} = 1.2$ m.

The refractive index is defined as $n(\mathbf{r}) = c_o/c(\mathbf{r}) \approx 1 - c'(\mathbf{r})/c_o$, where c_o and c' is the mean and fluctuating sound speed respectively, both dependent on temperature and

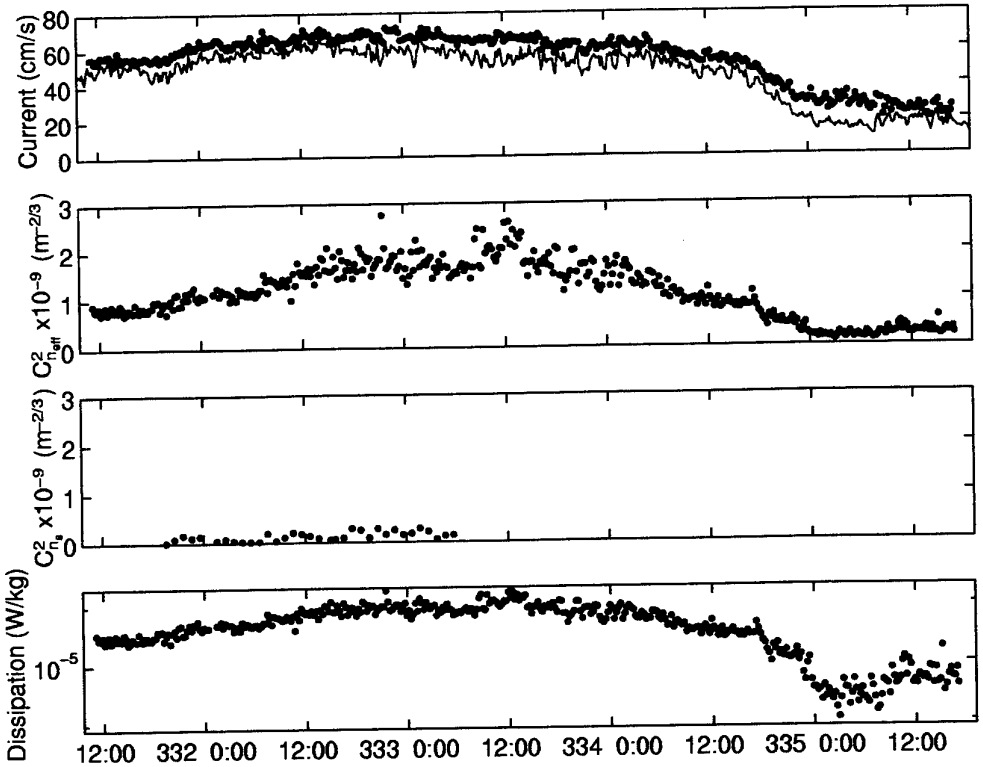

Figure 14 *Current speed from the ADCP together with the scintillation measurement, the effective structure parameter, the structure parameter for scalar refractive index fluctuations and the turbulent kinetic dissipation rate per unit mass.*

salinity (scalars). The refractive index fluctuations is then $\eta_s(\mathbf{r}) = -c(\mathbf{r})'/c_o$. Assuming isotropic and homogeneous turbulence the one-dimensional frequency spectrum for the refractive index fluctuations is defined as,

$$F_{\eta_s}(f) = 0.124 C_{\eta_s} (\frac{U}{2\pi})^{2/3} f^{-5/3}, \tag{12}$$

where C_{η_s} describes the level of the refractive index fluctuations from scalars and, U is the mean current speed advecting the small scale turbulence according to Taylor's hypothesis.

Figure 15 shows a sample sound speed time series sampled at 5 Hz evaluated from temperature and salinity taken at 60 m depth, with the one dimensional frequency spectrum for the refractive index fluctuations. A $-5/3$ slope is plotted to show that the variability can be modelled as described by (12) over the scales of interest. The

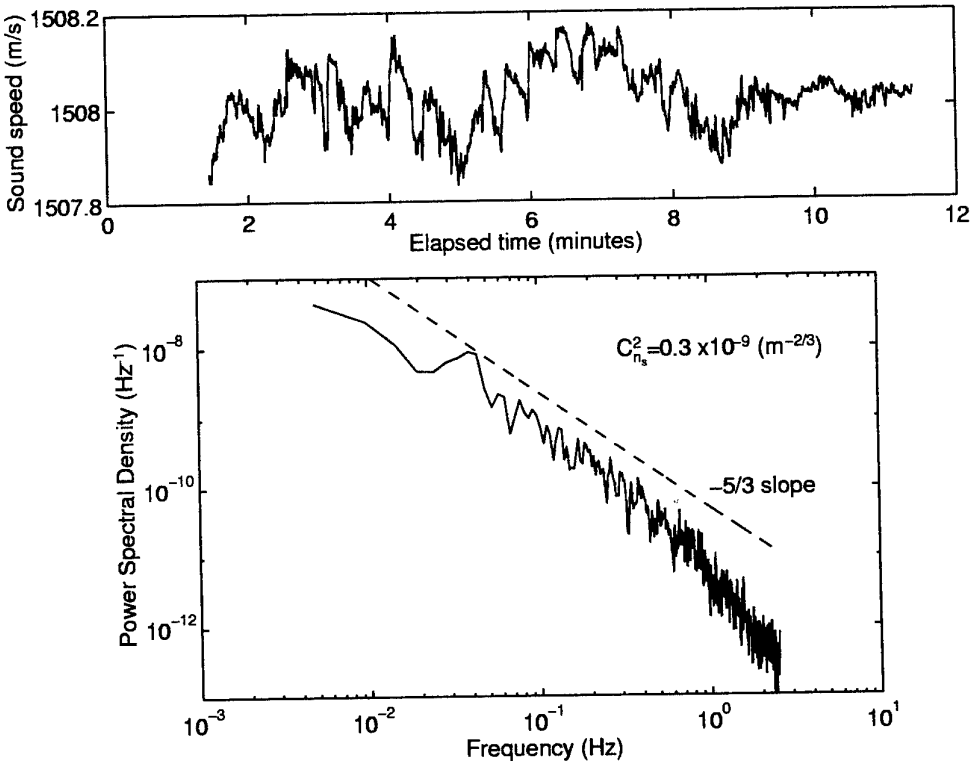

Figure 15 *A sample sound speed time series and the frequency spectrum for the refractive index fluctuations.*

level of the spectrum gives the structure parameter C_{η_s} which is compared to $C_{n_{eff}}^2$ in Fig. 14.

Independent measurements of the temperature / salinity structure compared with $C_{n_{eff}}^2$ in Fig. 14 show that the dominant acoustic scattering is from current velocity variability since $C_{n_s}^2$ is at most 10% of $C_{n_{eff}}^2$. The CTD measurement is sensitive to a minimum scale of 0.3 m whereas the acoustic measurement is sensitive to 1.2 m scales. Also the CTD measurement is at a point location and the acoustic measurement is a path average with weighting in the middle. Current velocity fluctuations arise because of hydrodynamic instability as discussed previously.

Since velocity fluctuations dominate the acoustic scattering, some interesting oceanographic parameters describing the turbulent boundary layer can be determined. For example the turbulent kinetic energy dissipation rate is determined by (see Di Iorio and Farmer [7]),

$$\epsilon^{2/3} = \frac{C_{n_v}^2 c_o^2}{1.97}. \tag{13}$$

The results are also shown in Fig. 14. Acoustic measurements of ϵ range from 1×10^{-6} to 1×10^{-4} $W\ kg^{-1}$. The dissipation of turbulent energy is also a measure of the production of turbulent energy caused by shear stresses and buoyancy forces. From Monin and Ozmidov [11] the balance is,

$$\frac{\tau_{xz}}{\rho_o}\frac{dU}{dz} + \frac{\tau_{yz}}{\rho_o}\frac{dV}{dz} - \frac{g}{\rho_o} < \rho' w' >= \epsilon. \tag{14}$$

where the shear stresses are defined by $\tau_{xz} = - < u'w' >$, $\tau_{yz} = - < v'w' >$ and the buoyancy flux is $< \rho' w' >$.

In estimating the bottom drag coefficient it is assumed that the dissipation rate calculated at 62.5 m, remains constant over the bottom boundary layer and that turbulent mixing forms a well mixed layer above the bottom so that the loss of energy by buoyancy is negligible. The flow close to the boundary is modelled as a log-layer as $dV/dz \approx 0$ and therefore, $\tau_{xz}/\rho_o \sim C_D U^2$. For a maximum dissipation rate of 1×10^{-4} $W\ kg^{-1}$ during maximum inflow, an estimated bottom drag coefficient is $C_D = 3.5 \times 10^{-3}$ which is consistent for a mixed sand and shell bottom.

6

Summary and Conclusions

This paper summarizes acoustic and oceanographic data collected during the 1995 sea trial in the Strait of Istanbul (Bosporus) and Black Sea exit region. Considerable spatial and temporal variability was observed in the Mediterranean flow into the Black Sea. Three properties of the Mediterranean flow were discussed. We have shown the path and spreading extent of the inflow together with the dilution, the geophysical processes which affect the Mediterranean flow and detailed measurements of the turbulent properties of the bottom boundary layer.

Extensive surveying with SWATH mapping showed that the Mediterranean flow is confined within a well defined canyon which initially is oriented in a Northeast direction and then turns toward the Northwest. During the SWATH mapping, simultaneous CTD profiles were obtained in order to measure the dilution of the Mediterranean effluent along the canyon. In addition, a 3.5 km grid of CTD profiles from NRV *Alliance* and TCG *Çubuklu* showed bottom salinity values of 30.3 very close to the continental slope, indicating that the dilution within the canyon and on the shelf was at most 6:36.

High resolution echo soundings gave two dimensional imaging of the two layer flow. Since the mixing between the two very different water masses is turbulent and biological matter tends to accumulate at the interface, a strong acoustic back scatter was obtained thus revealing detailed interfacial structure. The Mediterranean effluent was followed along the canyon and the shelf. Observations show that on the shelf, the Mediterranean flow exhibits a 'delta' like structure.

Moored ADCP measurements showed temporary but complete blockage of the Mediterranean undercurrent. This blockage was shown to correspond to times when the relative sea level difference was greater than 40 cm which corresponds to Black Sea transport exceeding $25 \times 10^3\ m^3\ s^{-1}$. The ADCP measurements also showed that the Mediterranean undercurrent exhibits Ekman-like spiral currents because of bottom and interfacial friction.

Profiles and time series of temperature and salinity at a fixed location showed substantial mixing between the Black Sea and Mediterranean water layers. This mixing was observed by a salinity increase of 0.5 in the Black Sea layer and a salinity decrease of 0.6 in the Mediterranean layer. This increase/decrease may be the result

of entrainment or advection of more saline/fresher water. The CTD profiles together with current velocity profiles gives a measure of hydrodynamic instability parameterized by the Richardson number. It was found that over the 36 h measurement period when the Mediterranean undercurrent was strong, the flow was consistently hydrodynamically unstable ($0 < \mathrm{Ri} < 0.25$).

The turbulent levels within the Mediterranean bottom boundary layer were observed using an acoustic scintillation instrument. Analysis of the acoustic amplitude showed increased variability with increasing current strength. The contribution of temperature and salinity variations to the total acoustic scattering was found to be negligible leading to the conclusion that the turbulent velocity variations dominated the acoustic scattering. This led to estimates of the path averaged, turbulent kinetic energy dissipation rate. Assuminga balance of production and dissipation of energy, estimates of the bottom drag coefficient gave $C_D = 3.5 \times 10^{-3}$.

7

Acknowledgements

The authors wish to thank the officers and crew of the NRV *Alliance* and TCG *Çubuklu* for their assistance in the collection of acoustic and oceanographic data. Many thanks to T. Akal and P. Guerrini for their expertise in acoustic systems. Thanks to J. Sellschopp for many help comments on the oceanographic analysis. Also thanks go to R. Della Maggiora and A. Brogini for their efforts in preparing the oceanographic instrumentation, G. Baldasserini for carrying out the preliminary oceanographic data processing. The SWATH processing was carried out by A. Trangeled and C. Sisti. Special thanks to D. Farmer of the Institute of Ocean Sciences, CANADA for lending us his acoustic scintillation and echo sounding instruments.

References

[1] D. Tolmazin. Changing coastal oceanography of the Black Sea. II: Mediterranean effluent. *Progress in Oceanography*, 15:277–316, 1985.

[2] Ü. Ünlüata, T. Oğuz, M.A. Latif, and E. Özsoy. On the physical oceanography of the Turkish Straits. In L.J. Pratt, editor, *The Physical Oceanography of Sea Straits*. Dordrecht, the Netherlands, Kluwer, 1990.

[3] H. Yüce. Investigation of the Mediterranean water in the Strait of Istanbul (Bosphorus) and the Black Sea. *Oceanologica Acta*, 13:177–186, 1990.

[4] H. Yüce. Mediterranean water in the Strait of Istanbul (Bosphorus) and the Black Sea exit. *Estuarine, Coastal and Shelf Science*, 43:597–616, 1996.

[5] M.A. Latif, E. Özsoy, T. Oğuz, and Ü. Ünlüata. Observations of the Mediterranean inflow into the Black Sea. *Deep-Sea Research*, 38:S711–S723, 1991.

[6] T. Oğuz, E. Özsoy, M. A. Latif, H. I. Sur, and Ü. Ünlüata. Modeling of hydraulically controlled exchange flow in the Bosphorus Strait. *Journal of Physical Oceanography*, 20:945–965, 1990.

[7] D. Di Iorio and D. M. Farmer. Path averaged turbulent dissipation measurements using high frequency acoustical scintillation analysis. *Journal of the Acoustical Society of America*, 96:1056–1069, 1994.

[8] L. Armi and D. M. Farmer. The flow of Mediterranean water through the Strait of Gibraltar. *Progress in Oceanography*, 21:1–105, 1988.

[9] D. M. Farmer and L. Armi. The flow of Atlantic water through the Strait of Gibraltar. *Progress in Oceanography*, 21:1–105, 1988.

[10] H. Yüce. On the variability of Mediterranean water flow into the Black Sea. *Continental Shelf Research*, 16:1399–1413, 1996.

[11] A.S. Monin and R.V. Ozmidov. *Turbulence in the Ocean*. Reidel, 1985.

[12] RD Instruments. In-situ acoustic scintillation flow sensor with application to hydrothermal vents SBIR: Phase II final report. Technical report, RDI N00014-88-C-0289, 1992.

[13] V. I. Tatarskii. *The Effects of the Turbulent Atmosphere on Wave Propagation*. Translated from Russian by Israel Program for Scientific Translations, Jerusalem, 1971.

[14] D. M. Farmer, S. F. Clifford, and J. A. Verrall. Scintillation structure of a turbulent tidal flow. *Journal of Geophysical Research*, 92:5369–5382, 1985.

[15] V. E. Ostachev. Sound propagation and scattering in media with random inhomogeneities of sound speed, density and medium velocity. *Waves in Random Media*, 4:403–428, 1994.

[16] D. Di Iorio and D. M. Farmer. Separation of current and sound speed in the effective refractive index for a turbulent environment using reciprocal acoustic transmission. *Journal of the Acoustical Society of America*, accepted for publication, 1997.

Document Data Sheet

NATO UNCLASSIFIED

Security Classification		Project No.
NATO UNCLASSIFIED		022-1
Document Serial No.	**Date of Issue**	**Total Pages**
SR-269	October 1997	41pp.

Author(s)

Di Iorio, D., Yüce, H.

Title

Observations of Mediterranean flow into the Black Sea

Abstract

Mediterranean Sea water inflow into the Black Sea is investigated using acoustic and oceanographic data obtained in the Black Sea exit region. The path of Mediterranean water and the resulting spreading on the continental shelf is observed with SWATH bottom bathymetry measurements, high resolution echo sounding images and conductivity, temperature and depth (CTD) profiles. It is found that the dilution of the saline Mediterranean water as it flows and spreads on the shelf is only 6.0 before reaching the continental slope where it sinks to a depth appropriate to its density. Temporal and spatial variability in the flow and their relation to atmospheric and sea level changes are documented. It is shown that blockage of the Mediterranean undercurrent occurs when the Black Sea water transport exceeds $25 \times 10^3\ m^3\ s^{-1}$ which corresponds to a relative sea level difference grater than 40 cm. Mediterranean flow into the Black Sea is a high Reynolds, low Richardson number flow resulting in a turbulent bottom boundary layer. Measurements of the path averaged turbulent kinetic energy dissipation rate give values ranging from 1×10^{-6} to $1\times10^{-4}\ W\ kg^{-1}$.

Keywords

Issuing Organization

North Atlantic Treaty Organization
SACLANT Undersea Research Centre
Viale San Bartolomeo 400, 19138 La Spezia, Italy

[From N. America: SACLANTCEN (New York) APO AE 09613]

Tel: +39 (0)187 540 111
Fax:+39 (0)187 524 600

E-mail: library@saclantc.nato.int

NATO UNCLASSIFIED

Initial Distribution for SR 269

Ministries of Defence

DND Canada	10
CHOD Denmark	8
DGA France	8
MOD Germany	15
HNDGS Greece	12
MARISTAT Italy	9
MOD (Navy) Netherlands	12
NDRE Norway	10
MOD Portugal	5
MDN Spain	2
TDKK and DNHO Turkey	5
MOD UK	20
ONR USA	42

NATO Commands and Agencies

NAMILCOM	2
SACLANT	3
CINCEASTLANT/ COMNAVNORTHWEST	1
CINCIBERLANT	1
CINCWESTLANT	1
COMASWSTRIKFOR	1
COMMAIREASTLANT	1
COMSTRIKFLTANT	1
COMSUBACLANT	1
SACLANTREPEUR	1
SACEUR	2
CINCNORTHWEST	1
CINCSOUTH	1
COMEDCENT	1
COMMARAIRMED	1
COMNAVSOUTH	1
COMSTRIKFORSOUTH	1
COMSUBMED	1
NC3A	1
PAT	1

Scientific Committee of National Representatives

SCNR Belgium	1
SCNR Canada	1
SCNR Denmark	1
SCNR Germany	1
SCNR Greece	1
SCNR Italy	1
SCNR Netherlands	2
SCNR Norway	1
SCNR Portugal	1
SCNR Spain	1
SCNR Turkey	1
SCNR UK	1
SCNR USA	2
French Delegate	1
SECGEN Rep. SCNR	1
NAMILCOM Rep. SCNR	1

National Liaison Officers

NLO Canada	1
NLO Denmark	1
NLO Germany	1
NLO Italy	1
NLO Netherlands	1
NLO Spain	1
NLO UK	1
NLO USA	1

Sub-total	208
SACLANTCEN	30
Total	238